Coherent beam-beam tune shift of unsymmetrical beam-beam interactions with large beam-beam parameter

Lihui Jin and Jicong Shi*
Department of Physics & Astronomy, The University of Kansas, Lawrence, Kansas 66045, USA

Georg H. Hoffstaetter
Department of Physics, Cornell University, Ithaca, New York 14850, USA
(Received 9 September 2004; published 21 March 2005)

Coherent beam-beam tune shift of unsymmetrical beam-beam interactions was studied experimentally and numerically in HERA, where the lepton beam has such a large beam-beam parameter (up to $\xi_y=0.272$) that the single-particle motion is locally unstable at the origin (closed orbit). Unlike the symmetrical case of beam-beam interactions, the ratio of the coherent beam-beam tune shift and the beam-beam parameter in this unsymmetrical case of beam-beam interactions was found to decrease monotonically with an increase of the beam-beam parameter. The results of self-consistent beam-beam simulation, the linearized Vlasov equation, and the rigid-beam model were compared with the experimental measurement. It was found that the coherent beam-beam tune shifts measured in the experiment and calculated in the simulation agree remarkably well but they are much smaller than those calculated by the linearized Vlasov equation with the single-mode approximation or the rigid-beam model. The study indicated that the single-mode approximation in the linearization of the Vlasov equation is not valid in the case of unsymmetrical beam-beam interactions. The rigid-beam model is valid only with a small beam-beam parameter in the case of unsymmetrical beam-beam interactions.

DOI: 10.1103/PhysRevE.71.036501 PACS number(s): 29.27.Bd, 29.20.−c, 05.45.−a

I. INTRODUCTION

To achieve a substantial increase of luminosity in a storage-ring collider, limited options include increase of bunch currents, reduction of beam sizes at interaction points (IPs), and increase of the number of colliding bunches. The first two measures unavoidably increase head-on beam-beam forces which could lead to collective (coherent) beam-beam instabilities [1,2]. Understanding of coherent beam-beam effects especially in the nonlinear regime is therefore of primary importance for achieving high luminosity in a storage-ring collider with high-intensity beams.

To study the coherent beam-beam effect, one important quantity that can be measured experimentally is the coherent beam-beam tune shift. Without beam-beam interactions and without considering nonlinearities in the lattice, the two counter-rotating beams oscillate transversely with frequencies that correspond to lattice tunes (betatron tunes without collision) if they deviate from close orbits. With beam-beam interactions, the particle distributions of the beams are perturbed and evolve with time according to the Vlasov equation [1]. The dynamics of the beams could therefore be complicated by multimode oscillations of the beam distributions. When considering only the stable oscillation of beam centroids (coherent dipole oscillation), the frequency spectrum of the beam-centroid oscillation has two primary frequencies for each degree of freedom of the transverse motion. These primary frequencies correspond to the tunes measured during collision. The differences between these measured collision tunes and the lattice tunes are the coherent beam-beam tune shifts [1,3,4]. Over decades, many studies have been conducted on the relationship between the coherent beam-beam tune shift and the beam-beam parameter that measures the strength of the beam-beam interaction [3–13]. Two theoretical models, the linearized Vlasov equation [1] and the rigid-beam model [5], have been studied extensively for cases of weak beam-beam perturbation in which the beam-beam parameter is relatively small. When the two beams have the same or very close lattice tunes, the calculation of the coherent beam-beam tune shift based on the linearized Vlasov equation with the single-mode approximation agrees with beam measurements and computer simulations [3,4,6,7]. The rigid-beam model is inconsistent with the linearized Vlasov equation and was therefore proven to be wrong by beam measurements in this case [6,7]. When the two beams have very different lattice tunes, on the other hand, the calculation based on the rigid-beam model provides a good agreement with beam measurements [5,8,14]. In both of these models, the equilibrium beam distributions were assumed to be Gaussian distributions for easing the calculations. In the case of weak beam-beam perturbation, this assumption is fairly good as the beams were observed to stay close to a Gaussian.

The situation of strong beam-beam perturbations with a relatively large beam-beam parameter is much more complicated and less understood. When the beam-beam parameter exceeds a threshold, the beam-beam interaction could induce a chaotic coherent beam-beam instability. After the onset of the instability, the closed orbits could become unstable for the beam centroids and two beams could develop a spontaneous unstable coherent oscillation [2,15]. When the beam-beam parameter is below the beam-beam threshold, the coherent beam oscillation is stable. It is, however, not clear

*Corresponding author. FAX: 785-864-5262; Email address: jshi@ku.edu

whether the linearized Vlasov equation or the rigid-beam model are still valid in the regime of strong beam-beam perturbation. As many efforts are being made to further increase the beam-beam parameter in upgrades of current and developments of future storage-ring colliders, an understanding of the coherent beam-beam tune shift in this regime is not only necessary for the interpretation of the tune measurement during operation of colliders with high-intensity beams, but also could shed light on the onset of the chaotic coherent beam-beam stability.

To explore the beam-beam effect with a large beam-beam parameter, a beam experiment, the HERA 2000 beam study, was performed on HERA [Hadron Electron Ring Accelerator at DESY (Deutsches Elektronen-Synchrotron), Hamburg, Germany] in which a 920 GeV proton (p) beam and a 27.5 GeV positron (e^+) beam collided at two IPs, H1 and ZEUS [16]. The beam-beam interaction in HERA is a typical case of unsymmetrical beam-beam interaction as the two beams have very different lattice tunes and beam-beam parameters (strong p beam and weak e^+ beam). In the experiment, the vertical beam-beam parameter of the e^+ beam was varied from 0.068 to 0.272 by changing the vertical beta function of the e^+ beam at two IPs. The emittance of the e^+ beam and the luminosity were measured as functions of the beam-beam parameter. One important phenomenon observed in this experiment is that the measured coherent beam-beam tune shifts of the e^+ beam are much smaller than those calculated from the rigid-beam model. This is the first experimental evidence indicating that the traditional models of the coherent beam-beam tune shift are no longer valid in the situation of strong beam-beam perturbations. It should be noted that in all the cases in the HERA experiment, the single-particle motion is locally unstable at the origin (closed orbit) due to beam-beam interactions. In the experiment, however, the beam was observed to have a very good lifetime and operation condition in all the cases. This is the first direct experimental observation of the global stability of a beam coexisting with the local instability of the beam particles due to beam-beam interactions.

To have a better understanding of the experimental data, we reconstructed the HERA beam experiment with a self-consistent beam-beam simulation. Remarkable agreement between the experiment and the simulation was observed on emittance growth and luminosity reduction. More significantly, the computer simulation confirmed the experimental result of very small coherent beam-beam tune shifts in this case of a very large beam-beam parameter. To examine the validity of the theoretical models for the coherent beam-beam tune shift, the linearized Vlasov equation and the rigid-beam model were solved for the HERA experiment. Since the distribution of the e^+ beam significantly deviated from the Gaussian due to the strong beam-beam interaction, the solutions of the linearized Vlasov equation and the rigid-beam model were calculated with the beam distributions obtained from the beam-beam simulation instead of assuming Gaussian distributions. It was found that for the unsymmetrical beam-beam interaction with a large beam-beam parameter, the result of the rigid-beam model is inconsistent with the beam experiment and beam simulation even though a more accurate beam distribution was used in the calculation. The coherent beam-beam tune shifts calculated from the linearized Vlasov equation with the single-mode approximation were also found to be significantly different from the result of the beam experiment and beam simulation regardless of whether the beam-beam parameter is large or small. As the linearization of the Vlasov equation is expected to be valid for at least a small beam-beam parameter, this discrepancy suggests that the single-mode approximation used for solving the linearized Vlasov equation may not be valid in the case of unsymmetrical beam-beam interactions. Unfortunately, without the single-mode approximation, the linearized Vlasov equation for the problem of beam-beam interactions is currently unsolvable computationally due to the unsolved degeneracy problem of a matrix with mode coupling.

This paper is organized as follows. Section II summarizes the results of the HERA 2000 beam experiment. In Sec. III, the self-consistent beam simulation for the HERA beam experiment is discussed. In Sec. IV, the coherent beam-beam tune shifts calculated by using the rigid-beam model or the linearized Vlasov equation are compared with the experiment/simulation results. The details of the coherent tune calculation with the theoretical models are presented in Appendixes A and B. The characteristics of the coherent beam-beam tune shift in the unsymmetrical case of beam-beam interactions are discussed in Sec. V. Section VI contains a summary remark.

II. HERA 2000 BEAM EXPERIMENT

In the luminosity upgrade of HERA, the beam-beam parameters of the electron beam have been nearly doubled. To examine any possible luminosity reduction due to beam-beam effects, a series of beam experiments were performed in HERA [14,16]. In the HERA 2000 beam experiment, the e^+ beam was used to collide with the p beam at the two IPs and the effect of a large beam-beam parameter of the lepton beam was explored by increasing the vertical beta function ($\beta_{e,y}$) of the e^+ beam at the IPs. The vertical beam-beam parameter ($\xi_{e,y}$) of the e^+ beam is related to $\beta_{e,y}$ by [17]

$$\xi_{e,y} = \frac{r_e N_p}{2\pi\gamma_e} \frac{\beta_{e,y}}{\sigma_{p,y}(\sigma_{p,x} + \sigma_{p,y})}, \tag{1}$$

where r_e and γ_e are the classic radius and Lorentz factor of positron, respectively, and N_p is the number of protons per bunch. The horizontal and vertical sizes of the p beam at the IPs are given by $\sigma_{p,x}$ and $\sigma_{p,y}$. In the experiment, the p beam current (I_p) was fixed. Since the beam-beam parameter of the p beam is very small, there was little change in the p beam size as it was observed during the experiment. The vertical beam-beam parameter $\xi_{e,y}$ is therefore linearly proportional to $\beta_{e,y}$ in this case. During the experiment, after the proton current was filled, $\xi_{e,y}$ was increased from 0.068 to 0.272 as $\beta_{e,y}$ was changed from 1.0 to 4.0 m while other lattice parameters were kept as constants. Table I lists some beam parameters used in the HERA experiment and Table II lists the e^+ beam current (I_e) and the beam-beam parameters of the e^+ and p beam at $\beta_{e,y}$ where the measurement was performed. The e^+ and p beam sizes were not matched during

TABLE I. Some beam parameters used in HERA 2000 beam experiment, where f_{rev} is the revolution frequency, N_{tot} and are the total number of bunches and the number of colliding bunches, I is the beam current, β_x and β_y are the horizontal and vertical beta function at the IPs, σ_x and σ_y are the horizontal and vertical beam size without collision at the IPs, ϵ_x and ϵ_y are the horizontal and vertical emittance without collision, ν_x and ν_y are the horizontal and vertical betatron tune, and τ_x and τ_y are the horizontal and vertical damping time.

Parameter	Positron beam (e^+)	Proton beam (p)
Energy (GeV)	27.5	920
f_{rev} (kHz)	47.317	47.317
N_{tot}/N_{col}	189/174	180/174
I (mA)	(see Table II)	90
β_x/β_y (m)	2.5/(see Table II)	7.0/0.5
σ_x/σ_y (μm)	283/(see Table II)	164/39.9
ϵ_x/ϵ_y (nm)	32.0/1.28	3.82/3.18
ν_x/ν_y	52.169/52.246	31.291/32.297
τ_x/τ_y (ms)	9.2/12.7	

the collision. Other accelerator parameters can be found in [16]. It should be noted that with two IPs in the HERA experiment, a beam-beam parameter of 0.272 is among the highest ever achieved in storage-ring colliders. It can be easily verified by using the transfer matrix with Courant-Snyder parameters that the single-particle dynamics of the e^+ beam including the beam-beam interactions is linearly unstable near the closed orbit. In the HERA experiment, however, the beam was observed to have a very good lifetime and operation condition even at $\xi_{e,y}=0.272$. As shown by the beam-beam simulation in the next section, the global stability of the e^+ beam is the result of the formation of a beam halo due to the beam-beam interactions.

In the experiment, the emittance of the e^+ beam and the luminosity were measured as functions of $\beta_{e,y}$ at both the IPs. In Figs. 1 and 2, the measured emittance and the specific luminosity were plotted, with discrete points, as functions of $\xi_{e,y}$. For each $\xi_{e,y}$ where the measurement was performed, two data points correspond to the measurement at the two IPs, respectively. The specific luminosity is defined as $\mathcal{L}_s = N_{col}\mathcal{L}/(I_e I_p)$, where N_{col} and $\mathcal{L}$ are the number of colliding bunches and the luminosity, respectively [14]. As shown in

TABLE II. The beam parameters that change with the vertical beta function ($\beta_{e,y}$) of the e^+ beam at the IPs in HERA 2000 beam experiment, where the subscripts e and p indicate the e^+ and p beam, respectively.

$\beta_{e,y}$ (m)	I_e (mA)	$\sigma_{e,y}$ (μm)	$\xi_{e,x}/\xi_{e,y}$	$\xi_{p,x}/\xi_{p,y}$ (10^{-4})
1.0	19	35.8	0.041/0.068	2.54/1.40
1.5	18	43.8	0.041/0.102	2.35/1.06
2.0	17	50.6	0.041/0.136	2.18/0.85
3.0	3.5	62.0	0.041/0.204	0.43/0.14
4.0	2.6	72.0	0.041/0.272	0.31/0.09

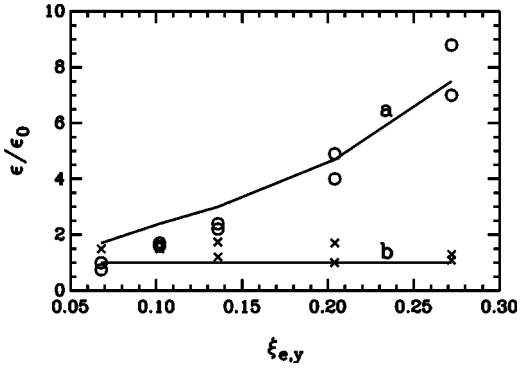

FIG. 1. Emittance of the e^+ beam as a function of $\xi_{e,y}$. ϵ_0 is the emittance without collision. Discrete points are from the experiment and continuous curves from the beam simulation. Circles and curve *a* are the vertical emittance. Crosses and curve *b* are the horizontal emittance. The two experimental data points at each $\xi_{e,y}$ where the measurement was performed correspond to the measurements at H1 and ZEUS.

Fig. 1, the vertical emittance growth of the e^+ beam increases monotonically and smoothly with the increase of $\xi_{e,y}$. This is the characteristics of the incoherent beam-beam effect, in contrast to the coherent beam-beam effect of which the emittance growth as a function of the beam-beam parameter could experience certain jumps (phase transitions) due to the onset of the coherent beam-beam instability [2]. To confirm that the luminosity reduction in Fig. 2 is indeed due to the emittance blowup, the luminosity calculated with the measured emittance by using the standard formula [16] is also plotted in Fig. 2. The agreement between the measured luminosity and the calculated luminosity in Fig. 2 shows a consistency in the emittance and luminosity measurement. In the experiment, the collision tunes of the e^+ beam were also measured at $\beta_{e,y}=4.0$ m as $\nu_x=52.160$ and $\nu_y=52.233$. The coherent beam-beam tune shift of the e^+ beam is therefore only $\Delta\nu_x=0.009$ and $\Delta\nu_y=0.013$, while from the rigid-beam model $\Delta\nu_x=0.016$ and $\Delta\nu_y=0.042$ if both the beams are Gaussian [14]. The measured coherent beam-beam tune shifts in this case are inconsistent with the traditional under-

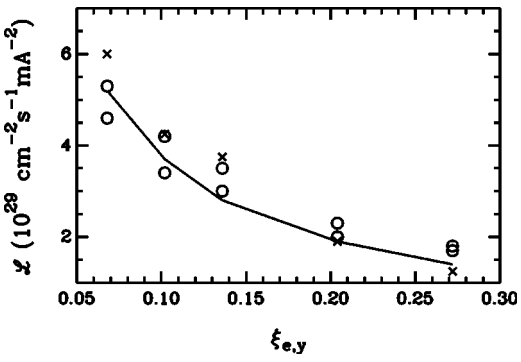

FIG. 2. The specific luminosity as a function of $\xi_{e,y}$. Circles are from the experiment and continuous curves from the beam simulation. The two experimental data points at each $\xi_{e,y}$ where the measurement was performed correspond to the measurements at H1 and ZEUS. Crosses are the luminosity calculated with the measured emittance in Fig. 1 assuming Gaussian beam distributions.

standing of beam coherent oscillation. Moreover, in the symmetrical case of beam-beam interactions, the ratio of the coherent beam-beam tune shift and the total beam-beam parameter has a value approximately ranging from 1.2 for round beams to 1.3 for flat (one-dimensional) beams [4], where the total beam-beam parameter is defined as the sum of the beam-beam parameter at each interaction point. In the HERA experiment, this ratio was found to be $\Delta\nu_{e,x}/(2\xi_{e,x})=0.11$ in the horizontal plane and $\Delta\nu_{e,y}/(2\xi_{e,y})=0.024$ in the vertical plane, respectively, for the e^+ beam at $\beta_{e,y}=4.0$ m. The coherent beam-beam tune shifts in this case of unsymmetrical beam-beam interactions with a large beam-beam parameter are therefore extremely small as compared with the symmetrical case of beam-beam interactions.

III. RECONSTRUCTION OF THE HERA BEAM EXPERIMENT WITH NUMERICAL SIMULATION

To have a better understanding of the measured data in the HERA experiment, we have reconstructed the experiment with a self-consistent beam-beam simulation. The computational code used in this study is an expanded version of [2] that is currently capable of studying beam-beam effects of hadron or lepton beams with any aspect ratio (ratio between vertical and horizontal beam size). In the simulation, the linear HERA lattice with the two IPs was used. The two colliding beams were represented by a million macroparticles with given initial Gaussian distributions in transverse phase space. Without beam-beam interactions, the initial beam distribution used in the simulation matches exactly with the lattice. Beam-beam interaction at each IP was represented by a kick in transverse phase space and the kick was calculated by using the particle-in-cell method as described in Ref. [2]. Since the beams in the HERA experiment were flat, a uniform mesh extending to $\pm 20\sigma$ in the configuration space with a grid constant of 0.2σ was necessary in this case. All the computational parameters in the code were carefully tested for the numerical convergence. Tracking of particle motion was conducted in four-dimensional transverse phase space without synchrotron oscillations and momentum deviations. For lepton beams, the quantum excitation and synchrotron damping were treated as kicks in each turn during the tracking. The horizontal kick is [18]

$$\Delta x = e^{-1/(2\tau_x)}x + [(1-e^{-1/(2\tau_x)})\epsilon_x]^{1/2}w_1,$$

$$\Delta p_x = e^{-1/(2\tau_x)}p_x + [(1-e^{-1/(2\tau_x)})\epsilon_x]^{1/2}w_2, \qquad (2)$$

where x and p_x are the normalized horizontal coordinate and its conjugate momentum, ϵ_x is the horizontal emittance, and w_1 and w_2 are random numbers with a Gaussian distribution that is centered at zero and has unit standard deviation. The damping time in the horizontal and vertical directions, τ_x and τ_y, has the unit of turns. For HERA, $\tau_x=436$ and $\tau_y=600$, respectively. The vertical kick has a similar formula.

With the beam-beam simulation, the emittance growth of the e^+ beam and the specific luminosity were calculated as functions of $\xi_{e,y}$ for the HERA experiment and the results were plotted in Figs. 1 and 2 as solid lines. Both the emittance and the luminosity plot show a remarkable agreement between the experiment and the simulation. Figure 3 plots the evolution of the vertical emittance of the e^+ beam at different $\beta_{e,y}$. In all these cases, after a quick emittance blowup, the beam emittance is restabilized and, consequently, an equilibrium (or quasiequilibrium) state of the e^+ beam was reached. A study of the motion of particles in the core of the e^+ beam showed that the single-particle motion is locally unstable at the origin due to beam-beam interactions and the vertical phase-space area in the vicinity of the origin is chaotic in all those cases. During the emittance blowup, the particles in the beam core escape quickly to the beam tails due to the local instability at the origin. Without the onset of the coherent beam-beam instability, on the other hand, the particles in the beam tails are stable for the beam-beam interaction. This restabilization of the beam emittance is therefore due to a depopulation of the beam core and formation of a beam halo. This is consistent with the experimental observation that the beam lifetime and operation conditions were good during the experiment even in the case of $\xi_{e,y}=0.272$ [16].

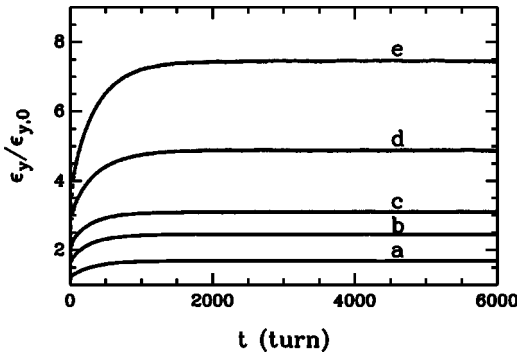

FIG. 3. Evolution of the vertical emittance of the e^+ beam calculated with the beam simulation for the cases of HERA beam experiment at (a) $\beta_{e,y}=1.0$ m; (b) $\beta_{e,y}=1.5$ m; (c) $\beta_{e,y}=2.0$ m; (d) $\beta_{e,y}=3.0$ m; and (e) $\beta_{e,y}=4.0$ m.

In the beam simulation, the coherent beam-beam tune shift was also calculated. Figure 4 is the calculated power spectrum of the coherent oscillation of the e^+ beam at $\beta_{e,y}=4.0$ m. Due to the quantum fluctuation, the e^+ beam always has a very small oscillation which is enough for the calculation of the coherent frequency if the numerical noise is small. Since a large number of particles were used for each of the beams, in this simulation the numerical noise was very low and we were able to calculate the coherent frequency without applying off-center kicks on the beams. The spectrum was calculated by the fast Fourier transformation (FFT) of the beam centroid motion from the 5000th to 9000th turn. Since at the 5000th turn the beam has already reached its quasiequilibrium, the transient state of the beam was thrown out during the tune calculation (see Fig. 3). As shown in Fig. 4, the power spectrum peaks at 0.1605 and 0.2331 in the horizontal and vertical planes, respectively, which corresponds to $\nu_x=52.161$ and $\nu_y=52.233$ for the beam coherent tunes during collision. This simulation result agrees excellently with the experimental measurement of $\nu_x=52.160$ and $\nu_y=52.233$. The beam-beam simulation therefore confirmed the coherent beam-beam tune shift measured in the HERA beam experiment.

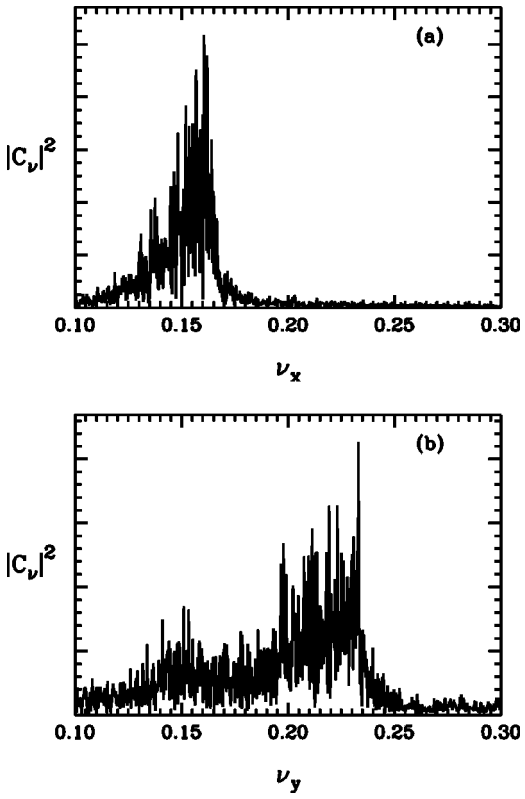

FIG. 4. Power spectrum of the centroid motion of the e^+ beam in (a) the horizontal and (b) the vertical direction for the case of HERA beam experiment at $\xi_{e,y}=0.272$ ($\beta_{e,y}=4.0$ m). The beam centroid motion was calculated during the beam simulation. Note that in this case the total beam-beam parameters for the two IPs are 0.082 and 0.544 in the horizontal and vertical plane, respectively.

The very small coherent beam-beam tune shift in this case of very large beam-beam parameter could be understood as the result of the depopulation of the beam core. To further confirm this, the dynamics of the beam particle distributions was studied during the beam simulation. Figure 5 plots the projection of the distribution in the vertical (y) direction and shows that the distribution of the e^+ beam deviates from a Gaussian distribution with a significant drop at the beam core and a growth of the beam tails. Due to the beam-beam interactions, the fixed point at the origin becomes unstable in the vertical phase space and bifurcates into a pair of new stable fixed points that locate symmetrically on the two sides of the origin and at a distance about $2\sigma_{e,y}$ from the origin, where $\sigma_{e,y}$ is the normalized vertical size of the e^+ beam without collision. Particles remaining inside the beam core are either chaotic or move around these two new fixed points in the vertical phase space. In the horizontal phase space, the particles in the beam core are still oscillating around the origin. Compared with the distribution of the e^+ beam, a Gaussian beam that has the same emittance of the e^+ beam has many more particles in the beam core. The real coherent beam-beam tune shift measured in the experiment and calculated with the beam simulation is therefore smaller than that calculated from the rigid-beam model with Gaussian beams. Moreover, the assumption of Gaussian beams in all the theoretical models of the coherent beam-beam oscillation neglects the effect of the ϕ dependence of the beam equilibrium distributions, where ϕ is the angle of the action-angle variable. In the HERA beam experiment, the equilibrium (quasiequilibrium) distribution of the e^+ beam in fact has a strong ϕ dependence as shown in Fig. 6. For a comparison, the initial distribution used in the simulation was also plotted in the figure and shows no ϕ dependence, as it should be. In order to compare the experimental/simulation result with calculations of theoretical models, the theoretical models need to be modified to include the ϕ dependence of non-Gaussian equilibrium distributions.

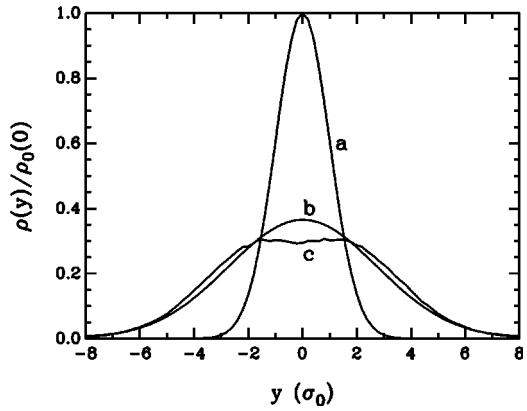

FIG. 5. The projection of the particle distribution of the e^+ beam in the vertical direction obtained by the beam simulation for the case of HERA beam experiment at $\xi_{e,y}=0.272$ ($\beta_{e,y}=4.0$ m). (a) The initial Gaussian distribution, (b) the distribution at the 5000th turn, and (c) the Gaussian distribution of which the standard deviation is the same as that of the beam distribution in (b).

To further insure the simulation code used in this study, we also tested our code on PEP-II, the B-factory at the Stanford Linear Accelerator Center. Beam-beam interactions in PEP-II are due to collisions between unsymmetrical electron (e^-) and positron beams. The luminosity and the collision tune calculated from the beam simulation were found to agree very well with the beam measurement performed on PEP-II [19,20]. For example, with the accelerator parameters given in Ref. [19], the calculated luminosity is 2.2

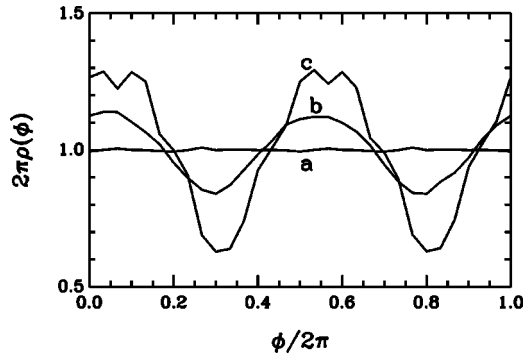

FIG. 6. The angle dependence of the particle distribution of the e^+ beam obtained by the beam simulation for the case of HERA beam experiment at $\xi_{e,y}=0.272$ ($\beta_{e,y}=4.0$ m). (a) The initial Gaussian distribution, (b) the ϕ_x dependence, and (c) the ϕ_y dependence of the distribution at the 5000th turn.

TABLE III. The coherent beam-beam tune shifts of the e^+ beam at $\beta_{e,y}=4.0$ m ($\xi_{e,y}=0.272$). "Experiment" and "Simulation" are the coherent tunes measured in the experiment and calculated in the beam simulation, respectively. "Rigid-Real" and "Rigid-Gaussian" are the coherent tunes calculated by using the rigid-beam model with a Gaussian distribution and with the distribution from the simulation, respectively. "Vlasov Eq." is the coherent tunes calculated with the linearized Vlasov equation.

$\beta_{e,y}=4.0$ m	$\nu_{e,x}$	$\Delta\nu_{e,x}/(2\xi_{e,x})$	$\nu_{e,y}$	$\Delta\nu_{e,y}/(2\xi_{e,y})$
Experiment	0.1600	0.110	0.2330	0.024
Simulation	0.1605	0.104	0.2331	0.024
Rigid-Real	0.1555	0.164	0.2194	0.049
Rigid-Gauss	0.1531	0.194	0.2040	0.077
Vlasov Eq.	0.1123	0.69		

$\times 10^{33}$ cm^{-2} s^{-1} when $I_{e^+}=1.1$ A and $I_{e^-}=0.61$ A while the measured luminosity is 2.1×10^{33} cm^{-2} s^{-1}. With the parameters given in Ref. [20], the horizontal collision tune of the e^- beam calculated from the beam simulation is 0.521 while the beam measurement is 0.524.

IV. VALIDITY OF THEORETICAL MODELS FOR BEAM COHERENT OSCILLATION

Two theoretical models, the rigid-beam model and the linearized Vlasov equation with the single-mode approximation, were examined with the HERA experiment. For the rigid-beam model, the coherent tunes were calculated with two different methods: assuming a Gaussian distribution as the equilibrium distribution of the e^+ beam [Eqs. (A10) and (A14) in Appendix A 1] or using the non-Gaussian quasiequilibrium distribution of the e^+ beam obtained in the beam-beam simulation (Appendix A 2). In the case of the Gaussian distribution, the beam sizes used in Eq. (A14) are of the experimental measurement or the beam-beam simulation. The small differences in the beam sizes measured in the experiment or calculated from the simulation (see Fig. 1) made little difference in Eq. (A14). For the linearized Vlasov equation, the horizontal coherent tunes were obtained by solving the initial-value problem of the linearized Vlasov equation with the single-mode approximation in the horizontal plane. The details of the calculations are in Appendixes A and B.

Tables III and IV list the ratio of the coherent beam-beam tune shifts and the total beam-beam parameters of the e^+ beam, $\Delta\nu_{e,x}/(2\xi_{e,x})$ and $\Delta\nu_{e,y}/(2\xi_{e,y})$, calculated in the beam simulation or calculated with the theoretical models for the cases of $\beta_{e,y}=1.0$ and 4.0 m, where $\Delta\nu_{e,x}$ and $\Delta\nu_{e,y}$ are the horizontal and vertical coherent beam-beam tune shift of the e^+ beam. The experimental measurement at $\beta_{e,y}=4.0$ m is also included in Table III. The significant discrepancy between the results of the models and the results of the experiment/simulation shows that the theoretical models are inconsistent with the experiment and simulation. Note that the rigid-beam model with the beam distribution from the simulation did a little better than that with Gaussian distribution. To further examine the failure of the theoretical models, a beam-beam simulation was conducted for the case of $\beta_{e,y}=1.0$ m but with only one-tenth of the p-bunch current used in the experiment, i.e., $\xi_{e,y}=0.0068$. The result is listed in Table V and shows that the rigid-beam model with either the Gaussian distribution or the distribution obtained from the simulation is in good agreement with the beam simulation. In fact, the quasiequilibrium distribution of the e^+ beam in this case is very close to a Gaussian. This reconfirms many previous studies that the rigid-beam model is correct for unsymmetrical beam-beam interactions with a relatively small beam-beam parameter. Contrary to the cases of the HERA experiment, in the case of $\xi_{e,y}=0.0068$ the single-particle dynamics including beam-beam interactions is stable at the origin (closed orbit). The failure of the rigid-beam models in the cases of the HERA experiment could therefore be due to the chaotic single-particle dynamics in the core of the e^+ beam.

TABLE IV. The same as Table III but for $\beta_{e,y}=1.0$ m ($\xi_{e,y}=0.068$).

$\beta_{e,y}=1.0$ m	$\nu_{e,x}$	$\Delta\nu_{e,x}/(2\xi_{e,x})$	$\nu_{e,y}$	$\Delta\nu_{e,y}/(2\xi_{e,y})$
Simulation	0.1600	0.110	0.2172	0.212
Rigid-Real	0.1517	0.212	0.2074	0.284
Rigid-Gauss	0.1475	0.263	0.1996	0.341
Vlasov Eq.	0.121	0.58		

TABLE V. The same as Table IV, but with only one-tenth of the p-bunch current used in the experiment ($\xi_{e,y}=0.0068$).

$\beta_{e,y}=1.0$ m	$\nu_{e,x}$	$\Delta\nu_{e,x}/(2\xi_{e,x})$	$\nu_{e,y}$	$\Delta\nu_{e,y}/(2\xi_{e,y})$
Simulation	0.1672	0.224	0.2414	0.337
Rigid-Real	0.1668	0.263	0.2406	0.396
Rigid-Gauss	0.1668	0.268	0.2406	0.399
Vlasov Eq.	0.165	0.53		

In the case of the linearized Vlasov equation, as shown in Tables III–V, the calculation yielded wrong results no matter how small the beam-beam parameter is. In the calculation with the Vlasov equation, several approximations were employed. Among them, the linearization, the one-dimensional beam, and the single-mode approximation are the three major approximations that cannot be directly justified by the experimental observations (see Appendix B). The linearization of the Vlasov equation should not play the leading role in its failure for the unsymmetrical beam-beam interaction since the linearization should be valid for a relatively small beam-beam parameter. To verify the validity of the one-dimensional approximation, we did a series of beam-beam simulations for the case of $\beta_{e,y}=1.0$ m, $\xi_{e,y}=0.068$ or 0.0068, but with a different beam aspect ratio ($\sigma_{y,e}/\sigma_{x,e}$) ranging from 0.063 to 0.120. In all these cases, the horizontal coherent beam-beam tune shift was found to be very similar to that of the HERA experiment. Note that in the HERA experiment and in all the cases in Tables III–V, $\sigma_{y,e}/\sigma_{x,e}=0.126$. This indicates that the horizontal coherent beam-beam tune shift is not sensitive to the aspect ratio of the beam. A similar

phenomenon has also been observed in the symmetrical case of beam-beam interactions [4]. The large discrepancy in the coherent beam-beam tune shifts calculated with the linearized Vlasov equation as compared to that obtained from the experiment/simulation is apparently not due to the approximation of the one-dimensional beam. With the single-mode approximation, on the other hand, the only oscillation mode of the beam distribution that was kept in the calculation is the $m=1$ mode in Eq. (B6). As shown in Fig. 6, the equilibrium distribution of the e^+ beam [$f_{1,0}(I,\phi)$ in Eq. (B4)] depends strongly on ϕ. In this case, the dominant mode of the equilibrium distribution is the $m=2$ mode, which has a ϕ dependence of $e^{i2\phi}$. As the $m=2$ mode could be a dominant intrinsic mode of the system, the single-mode approximation could be inconsistent with the dynamics of the beam. In order to study the effect of mode couplings in the linearized Vlasov equation, we have derived the eigenvalue equation of the linearized Vlasov equation that is similar to Eq. (B13) but includes high-order modes. After truncating higher-order modes at $m=m_p$, $\mathbf{M}$ in Eq. (B13) becomes a $(2m_p+1)(2l_p+2)\times(2m_p+1)(2l_p+2)$ matrix where l_p is the number of grids on the mesh of the action space and $\mathbf{M}_1$ and $\mathbf{M}_2$ in Eq. (B14) are no longer diagonal matrices (see Appendix B). We have, however, failed in obtaining a set of orthogonal eigenvectors for the eigenvalue equation of the linearized Vlasov equation because $\mathbf{M}$ is a singular (ill-conditioned) matrix when the mode couplings are included. A similar problem has also been encountered when including the mode coupling in the case of symmetrical beam-beam interactions.

V. COHERENT BEAM-BEAM TUNE SHIFT VERSUS BEAM-BEAM PARAMETER

In the symmetrical case of beam-beam interactions, the ratio of the coherent beam-beam tune shift and the total beam-beam parameter is approximately a constant of 1.2 for round beams and 1.3 for flat beams [4]. Note that with symmetrical beam-beam interactions, the beam-size growths of the two beams are symmetrical and the beam distributions are usually close to a Gaussian when the beam-beam parameter is below the threshold of the onset of coherent beam-beam instability [2,15]. The coherent beam-beam tune shift thus depends linearly on the beam-beam parameter in a fairly large range of beam-beam parameter [4]. On the contrary, in the HERA experiment the ratio of the coherent beam-beam tune shift and the beam-beam parameter of the e^+ beam decreases monotonically with the increase of the beam-beam parameter as shown in Fig. 7. This different characteristic of the coherent beam-beam tune shift stems mainly from the mismatch in the equilibrium distributions of two unsymmetrical colliding beams. In the HERA experiment, the beam size of the e^+ beam at the IPs is slightly larger than that of the p beam initially without collision (see Table I). When the beam-beam parameter is small such as in the case of $\xi_{e,y}=0.0068$, the beam-size growth is insignificant and the beams are very close to the initial Gaussian distributions. The ratio of the coherent beam-beam tune shift and the beam-beam parameter of the e^+ beam is simply determined by the mismatch in the initial beam sizes without collision as described by Eq. (A14) of the rigid-beam model. When the beam-beam parameter is large, on the other hand, the equilibrium size of the e^+ beam is much larger than that of the p beam and the beam-size growth of the e^+ beam (see Fig. 1) dominates the beam-size mismatch. Moreover, the particle distribution of the e^+ beam deviates significantly from a Gaussian distribution (see Fig. 5). In this case, the origin (closed orbit) of the phase space of the e^+ beam is unstable for the single-particle motion and a large number of positrons initially in the core of the e^+ beam escape to the beam tails and form a halo near the tail of the p beam. The coherent beam-beam tune shift of the e^+ beam thus becomes much smaller than that in the case of two matched Gaussian beams. Note that for two matched Gaussian beams, the ratio of the coherent beam-beam tune shift and the total beam-beam parameter is 0.5 for unsymmetrical beam-beam interactions. For the e^+ beam in the HERA experiment, as the beam-size growth and the resultant beam-size mismatch increase with the beam-beam parameter, the ratio of the coherent beam-beam tune shift and the beam-beam parameter decreases with the beam-beam parameter. In general, in the unsymmetrical case of beam-beam interactions, the two colliding beams have different equilibrium distributions described as the equilibrium states of the Vlasov equation in Eq. (B4). The mismatch in the distributions as well as the beam sizes is, in principle, independent of the initial states of the beam distributions and the initial beam-size mismatch as long as the considered equilibrium state of the Vlasov equation is well isolated and is the only one that is close to the initial beam distributions. The beam-size mismatch in the unsymmetrical case of beam-beam interactions is therefore intrinsic and unavoidable, especially when the beam-beam parameter is larger. Moreover, this beam-size mismatch increases with the strength of beam-beam perturbations. The functional dependence of the coherent beam-beam tune shift on the beam-beam parameter in Fig. 7 is therefore a general characteristic of unsymmetrical beam-beam interactions.

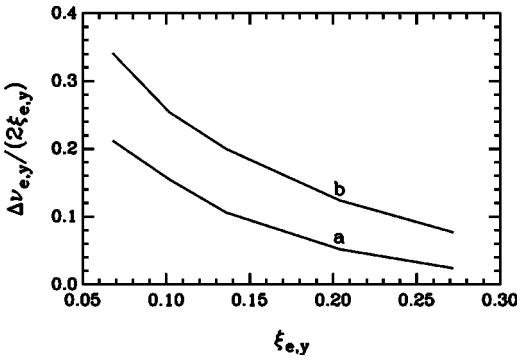

FIG. 7. The ratio of the coherent beam-beam tune shift and the beam-beam parameter as a function of the beam-beam parameter of the e^+ beam in the vertical plane calculated from (a) the beam-beam simulation and (b) the rigid-beam model with the Gaussian distribution.

Figure 7 also plots $\Delta\nu_{e,y}/(2\xi_{e,y})$ as a function of $\xi_{e,y}$ calculated based on the rigid-beam model. It shows that when the beam-beam parameter is large, the rigid-beam model results in a similar $\xi_{e,y}$ dependence of $\Delta\nu_{e,y}/(2\xi_{e,y})$ even

though it overestimates the coherent beam-beam tune shift. Note that in the rigid-beam model, this $\xi_{e,y}$ dependence is due to the beam-size mismatch as given in Eq. (A14). At a large $\xi_{e,y}$, the beam-size mismatch is dominated by the beam-size growth of the e^+ beam. This suggests that the result of the rigid-beam model in Eq. (A14) provides an approximation of the functional dependence of the coherent beam-beam tune shift to the intrinsic beam-size mismatch in unsymmetrical beam-beam interactions with large beam-beam parameters. The overestimate of the rigid-beam model could be due to the chaotic dynamics of the particles in the beam core. The linearization in theoretical models usually distorts the characteristics of the chaotic dynamics of a nonlinear system. The importance of the chaotic single-particle dynamics in the beam core to the beam coherent motion is, however, not very clear and needs to be further studied.

VI. CONCLUSION

The coherent beam-beam tune shift was studied in the case of unsymmetrical beam-beam interactions where the two beams have very different beam-beam parameters and betatron tunes. The results of a self-consistent beam-beam simulation, the rigid-beam model, and the linearized Vlasov equation were compared with the beam measurement in the HERA 2000 Beam Study. Remarkable agreement was found between the beam simulation and the HERA experiment in a wide range of, and, especially, at very large beam-beam parameters of, the lepton beam. The rigid-beam model was found to be only correct when the beam-beam parameter is small. The result of the linearized Vlasov equation with the single-mode approximation is inconsistent with the result of the beam experiment/simulation in either cases of large or small beam-beam parameter. The failure of the linearized Vlasov equation could be due to the single-mode approximation used in solving the linearized Vlasov equation. A study of the dynamics of the beam distribution showed that the high-order modes are important to the beam dynamics in this situation. An attempt to include high-order modes in the calculation has, however, not been successful because of the difficulty in finding a set of orthogonal eigenvectors for the linearized Vlasov equation. Recently, efforts have been made to include the angle dependence of beam distributions in an expansion of the Vlasov equation [21]. More studies are needed for a relevant solution of the linearized Vlasov equation for the unsymmetrical beam-beam interaction. Currently, the numerical simulation is the only reliable approach for a prediction of the coherent beam-beam tune shift in this situation.

One interesting phenomenon observed in this study is the very small coherent beam-beam tune shift in this unsymmetrical case of beam-beam interactions. It was found that the ratio of the coherent beam-beam tune shift and the total beam-beam parameter of the weak lepton beam in HERA decreases from 0.3 to 0.02 as the total beam-beam parameter increases from 0.01 to 0.54. On the contrary, in the symmetrical case of beam-beam interactions, this ratio maintains approximately a constant of 1.2 for a round beam or 1.3 for a flat beam in a large range of beam-beam parameter. The reason for this different characteristic of the coherent beam-beam tune shift is the intrinsic beam-size mismatch between two unsymmetrical colliding beams due to the difference in the equilibrium distributions of the two beams. This intrinsic mismatch in the beam distributions due to beam-beam interactions becomes more pronounced as the strength of beam-beam perturbations increases. The ratio of the coherent beam-beam tune shift and the beam-beam parameter decreases, in general, with the increase of beam-beam parameters in the unsymmetrical case of beam-beam interactions.

ACKNOWLEDGMENTS

This work is supported by the U.S. Department of Energy under Grant No. DE-FG02-04ER41288. The authors would like to thank the Center for Advanced Scientific Computing at the University of Kansas for the use of the Supercomputer. The authors thank F. Willeke and S. Peggs for many stimulating discussions. The authors would also like to thank Y. Cai for the help on the benchmark of our simulation code with the PEP-II beam simulation and measurement. J.S. would also like to thank DESY for the financial support for a trip to DESY at an early stage of our collaboration.

APPENDIX A: COHERENT BEAM-BEAM TUNE SHIFT FROM THE RIGID-BEAM MODEL

The coherent beam-beam tune shift in the rigid-beam model has been studied before for the unsymmetrical beam-beam interaction. Previous studies are, however, limited to the special cases where either the two beams have the same [8] or very different [14] beam-beam parameters. Moreover, all of them assumed that the beams are Gaussian. In the following, a general formula of the rigid-beam model is derived that can be applied to any case of unsymmetrical beam-beam interaction with either Gaussian or non-Gaussian beams.

Let $\rho_i(\vec{r},\theta)$ be the distribution of beam i in the normalized configuration space where $i=1$ or 2, $\vec{r}=(x,y)$ are the normalized coordinates of the transverse space, and θ is the azimuthal angle associated with the path length along the closed orbit. The beam centroid in the normalized space can be calculated by $\vec{R}_i=\int \vec{r}\rho_i(\vec{r},\theta)d\vec{r}$. Considering a linear lattice with one IP, the transverse motion of the beam centroid can be described by

$$\frac{d^2\vec{R}_i}{d\theta^2}+\mathbf{\Omega}_i\cdot\vec{R}_i=(-1)^{i+1}\lambda_i\vec{F}\left[2\pi\sum_n \delta(\theta-2\pi n)\right]. \quad \text{(A1)}$$

In Eq. (A1), $\mathbf{\Omega}_i$ is a 2×2 diagonal matrix with $(\mathbf{\Omega}_i)_{11}=\nu_{i,x}^2$ and $(\mathbf{\Omega}_i)_{22}=\nu_{i,y}^2$, where $(\nu_{i,x},\nu_{i,y})$ are the fractional parts of the betatron tunes of the lattice for beam i. The main part of the beam-beam kick in Eq. (A1) is

$$\vec{F}=\int_{-\infty}^{+\infty}\int_{-\infty}^{+\infty}\rho_1(\vec{r}_1,\theta)\rho_2(\vec{r}_2,\theta) \times\vec{G}(\beta_{1,x}^{1/2}x_1-\beta_{2,x}^{1/2}x_2,\beta_{1,y}^{1/2}y_1-\beta_{2,y}^{1/2}y_2)d\vec{r}_1d\vec{r}_2, \quad \text{(A2)}$$

where $\vec{G}(x,y)=\vec{r}/r^2$ is the Green function of the beam-beam

interaction and $(\beta_{i,x},\beta_{i,y})$ are the horizontal and vertical beta function of beam i at the IP, respectively. The strength of the beam-beam kick for the horizontal component of Eq. (A1) is

$$\lambda_i = \lambda_{i,x} = \frac{a_i N_j}{\pi\gamma_i}\nu_{i,x}\beta_{i,x}^{1/2},$$

where $i=1$ or 2, $j=1$ or 2, but $i\neq j$; N_j is the number of particles per bunch of beam j; a_i is the classical radius of the particle in beam i; and γ_i is the Lorentz factor of beam i. With the definition of the beam-beam parameters in Eq. (1), this kick strength can be written as

$$\lambda_{i,x} = \frac{2\nu_{i,x}\xi_{i,x}}{\beta_{i,x}^{1/2}}\sigma_{j,x}(\sigma_{j,x}+\sigma_{j,y}), \tag{A3}$$

where $(\xi_{i,x},\xi_{i,y})$ and $(\sigma_{i,x},\sigma_{i,y})$ are the beam-beam parameters and the rms beam sizes at the IP of beam i. For the vertical component of Eq. (A1), $\lambda_i=\lambda_{i,y}$ can be easily obtained by exchanging x and y in Eq. (A3).

In the rigid-beam model of the coherent beam-beam oscillation, the shapes of the particle distributions in phase space are assumed not to change with time during the beam oscillation while the centers of the distributions oscillate with the beams' coherent tunes. The distribution during the beam oscillation is thus assumed to be $\rho_i(\vec{r},\theta)=\rho_{0i}(\vec{r}-\vec{R}_i)$, where $\rho_{0i}(\vec{r})$ is the equilibrium distribution when the beam is centered at the closed orbit. In general, $\vec{F}$ in Eq. (A2) is a function of moments of phase-space variables and the time dependence of $\vec{F}$ is implicitly through all the moments. (To have a better picture of this, one may consider a moment expansion of beam particle distributions in phase space.) With the rigid-beam approximation, $\vec{F}$ depends on the lowest-order moments $\vec{R}_1$ and $\vec{R}_2$ only,

$$\vec{F} = \int_{-\infty}^{+\infty}\int_{-\infty}^{+\infty}\rho_{01}(\vec{r}_1-\vec{R}_1)\rho_{02}(\vec{r}_2-\vec{R}_2) \times\vec{G}(\beta_{1,x}^{1/2}x_1-\beta_{2,x}^{1/2}x_2,\beta_{1,y}^{1/2}y_1-\beta_{2,y}^{1/2}y_2)d\vec{r}_1 d\vec{r}_2. \tag{A4}$$

Note that the rigid-beam model may fail in cases where the variation of the distributions is important during the beam coherent oscillation. To find the oscillation frequencies of $\vec{R}_i$, one can average the beam-beam kick in Eq. (A1) over one turn (2π in the longitudinal direction) and expand $\vec{F}$ into a Taylor series of $\vec{R}_i$. Keeping only the linear terms of $\vec{R}_i$, Eq. (A1) becomes a coupled four-dimensional harmonic oscillator,

$$\frac{d^2\vec{R}_i}{d\theta^2} + \mathbf{\Omega}_i\cdot\vec{R}_i = (-1)^{i+1}\lambda_i(\mathbf{A}_1\cdot\vec{R}_1+\mathbf{A}_2\cdot\vec{R}_2), \tag{A5}$$

where $i=1$ or 2, and $\mathbf{A}_i$ are 2×2 matrices with

$$\mathbf{A}_i = \left.\frac{\partial\vec{F}}{\partial\vec{R}_i}\right|_{\vec{R}_1=0,\vec{R}_2=0}. \tag{A6}$$

If both the beams are mirror symmetric with respect to the horizontal and vertical plane, $\mathbf{A}_i$ are diagonal matrices and the horizontal and vertical coherent oscillations are decoupled. The two eigenfrequencies for the coherent oscillation in the horizontal plane can then be solved as

$$\nu_\pm = \frac{1}{\sqrt{2}}\sqrt{\omega_1^2+\omega_2^2 \pm \sqrt{(\omega_1^2-\omega_2^2)^2+16\nu_{1,x}\nu_{2,x}\delta\omega_1\delta\omega_2}}, \tag{A7}$$

where

$$\omega_i^2 = \nu_{i,x}^2 - 2\nu_{i,x}\delta\omega_i,$$

$$\delta\omega_i = \lambda_{i,x}(\mathbf{A}_i)_{11}/(2\nu_{i,x}) \tag{A8}$$

for $i=1$ or 2. If $\delta\omega_i \ll \nu_{i,x}$ and in Eq. (A7)

$$(\omega_1^2-\omega_2^2)^2 \gg 16\nu_{1,x}\nu_{2,x}\delta\omega_1\delta\omega_2, \tag{A9}$$

then the coherent frequencies of the two beam are

$$\nu_+ = \omega_1 = \nu_{1,x} - \delta\omega_1,$$

$$\nu_- = \omega_2 = \nu_{2,x} - \delta\omega_2, \tag{A10}$$

where ν_+ and ν_- are the horizontal coherent tunes of beam 1 and beam 2, respectively. Note that in the unsymmetrical case of beam-beam interactions, the two eigenfrequencies do not correspond to the so called 0 (or σ) and π modes of symmetrical beam-beam interactions. The condition in Eq. (A9) can be further simplified as

$$|\nu_{1,x}-\nu_{2,x}| \gg \sqrt{\delta\omega_1\delta\omega_2}. \tag{A11}$$

Therefore, if the difference of the lattice tunes is much larger than the geometric average of the coherent beam-beam tune shifts of the two beams, the coherent beam-beam tune shifts can simply be calculated with Eq. (A10). Note that in the HERA experiment, this condition was fulfilled. For the case of strong-weak beam-beam interactions such as $\xi_{1,x}\gg\xi_{2,x}$, one can expand $\nu_\pm$ in terms of $\lambda_{2,x}/\lambda_{1,x}$. Keeping only the dominant term in the coherent beam-beam tune shifts yields

$$\nu_+ = \nu_{1,x} - \delta\omega_1,$$

$$\nu_- = \nu_{2,x} - \frac{\nu_{1,x}^2-\nu_{2,x}^2}{\nu_{1,x}^2-\nu_{2,x}^2-2\nu_{1,x}\delta\omega_1}\delta\omega_2, \tag{A12}$$

where ν_+ and ν_- are the coherent frequencies of the weak (beam 1) and strong (beam 2) beam, respectively. In the first equation of Eq. (A12), since the zeroth-order term $(\delta\omega_1)$ of $\lambda_{2,x}/\lambda_{1,x}$ exists and dominates the coherent beam-beam tune shift of beam 1, the first- or higher-order terms were neglected. In the second equation of Eq. (A12), on the other hand, the zeroth-order term is zero and the first-order term was thus kept. Note that if the lattice tunes of the two beams are very different, Eq. (A12) is equivalent to Eq. (A10). If the denominator in Eq. (A12), $\nu_{1,x}^2-\nu_{2,x}^2-2\nu_{1,x}\delta\omega_1$, is small, an analysis of the higher-order terms shows that the expansion in terms of $\lambda_{2,x}/\lambda_{1,x}$ is no longer accurate and the coherent tunes have to be calculated by using Eq. (A7). The two coherent frequencies in the vertical plane can be easily obtained by exchanging x and y and changing $(\mathbf{A}_i)_{11}$ with $(\mathbf{A}_i)_{22}$ in Eqs. (A7)–(A12). As shown in our study (see Sec.

IV), this approach of the rigid-beam model is quite good in the case of unsymmetrical beam-beam interactions with a small beam-beam parameter.

1. Gaussian beams

In the case that ρ_{0i} are Gaussian distributions, matrix $\mathbf{A}_i$ in Eq. (A6) can be calculated analytically with Eq. (A4) as

$$(\mathbf{A}_i)_{11} = \frac{\beta_{i,x}^{1/2}}{\Sigma_x(\Sigma_x + \Sigma_y)}, \tag{A13}$$

where $\Sigma_x = \sqrt{\sigma_{1,x}^2 + \sigma_{2,x}^2}$ and $\Sigma_y = \sqrt{\sigma_{1,y}^2 + \sigma_{2,y}^2}$. The matrix element of $(\mathbf{A}_i)_{22}$ can be simply obtained by exchanging x and y in Eq. (A13). Substituting Eqs. (A2) and (A13) into Eq. (A8) yields

$$\delta\omega_i = \xi_{i,x}\frac{(\sigma_{j,x} + \sigma_{j,y})\sigma_{j,x}}{(\Sigma_x + \Sigma_y)\Sigma_x}, \tag{A14}$$

where $i=1$ or 2, $j=1$ or 2, but $j \neq i$. When $i=1$, Eq. (A14) gives the coherent beam-beam tune shifts of the weak beam [beam 1 in Eq. (A12)] obtained previously by Hoffstaetter for the strong-weak case of beam-beam interactions [14]. If $(\nu_{1,x}, \nu_{1,y}) = (\nu_{2,x}, \nu_{2,y})$ and $(\sigma_{1,x}, \sigma_{1,y}) = (\sigma_{2,x}, \sigma_{2,y})$, Eq. (A7) is reduced to the formula obtained by Hirata [5]. If $(\xi_{1,x}, \xi_{1,y}) = (\xi_{2,x}, \xi_{2,y})$ and $(\sigma_{1,x}, \sigma_{1,y}) = (\sigma_{2,x}, \sigma_{2,y})$, Eq. (A7) is reduced to the formula obtained by Hofmann [8].

2. Non-Gaussian beams

For non-Gaussian beams, especially the distributions obtained from beam-beam simulations such as that in Figs. 5 and 6, matrices $\mathbf{A}_i$ in Eq. (A6) cannot be obtained analytically but can be calculated numerically by using Eq. (A4). The coherent frequencies can then be calculated with Eq. (A7) or directly from Eq. (A5) if the horizontal and vertical motions are coupled.

APPENDIX B: COHERENT BEAM-BEAM TUNE SHIFT FROM THE LINEARIZED VLASOV EQUATION

The use of the linearized Vlasov equation has been very successful for the coherent beam-beam tune shift in the case that two beams have the same or very close lattice tunes [4]. In order to find the coherent beam-beam tune shift, one needs to identify the coherent frequencies from the eigenfrequencies of the linearized Vlasov equation. The linearized Vlasov equation, in principle, has infinite numbers of eigenfrequencies associated with infinite numbers of oscillation modes. For real beams, the number of the eigenfrequencies of the beam oscillation in transverse space is twice the number of particles in a bunch. When two beams have the same lattice tunes, the coherent frequencies can be easily identified since the eigenfrequencies that correspond to the coherent frequencies are separated from the rest of the eigenfrequencies that form a continuous band (many close eigenfrequency lines) [4], although it is not very clear mathematically why this separation occurs. The situation becomes more complicated when two beams have very different lattice tunes. In this case, all the eigenfrequencies are in one or two continuous bands and the coherent frequencies cannot be identified by only solving the eigenfrequencies. In order to find the coherent frequencies in the HERA beam experiment, we will instead solve the initial-value problem of the linearized Vlasov equation for the coherent beam oscillation.

Consider only the horizontal motion (very flat beam) in a linear lattice with one IP. In terms of the action-angle variable, the Hamiltonian for the betatron motion of beam i ($i=1$ or 2) can be written as

$$H_i(I,\phi,\theta) = H_{i,0}(I) + U_i(I,\phi,\theta)\left[2\pi\sum_n \delta(\theta - 2\pi n)\right], \tag{B1}$$

where $H_{i,0} = \nu_{i,x}I$ is the Hamiltonian associated with the betatron motion in the linear lattice and U_i is the potential energy for the beam-beam interaction that can be written, for one-dimensional beams, as

$$U_i(I,\phi,\theta) = U_i[f_j] = -2\frac{\xi_{i,x}\sigma_{j,x}^2}{\beta_{i,x}}\int_0^{2\pi}\int_0^{\infty} f_j(I',\phi',\theta) \times \ln(\sqrt{2\beta_{i,x}I}\sin\phi - \sqrt{2\beta_{j,x}I'}\sin\phi')dI'd\phi', \tag{B2}$$

where $i=1$ or 2 and $j=1$ or 2, but $i \neq j$. The action-angle variables are related to the normalized variables by $x = \sqrt{2I}\sin\phi$ and $p = \sqrt{2I}\cos\phi$. $f_i(I,\phi,\theta)$ is the particle distribution of beam i in phase space and satisfies the Vlasov equation. For convenience, we also define a functional $U_i[f_j]$ in Eq. (B2) for the potential integral. In Eq. (B2), $\ln(x-x')$ is the Green function for the potential of beam-beam interaction in one-dimensional space. If only the coherent beam-beam tune shifts are involved, one can get rid of the periodic δ function in the Hamiltonian in Eq. (B1) by averaging the beam-beam force over one turn. The Vlasov equation for f_i can then be written as

$$\frac{\partial f_i}{\partial\theta} + \nu_{i,x}\frac{\partial f_i}{\partial\phi} = \{U_i, f_i\}, \tag{B3}$$

where $\{\}$ is the Poisson bracket. Assume that the beams have reached equilibrium distributions $f_{i,0}$ that satisfy

$$\nu_{i,x}\frac{\partial f_{i,0}}{\partial\phi} = \{U_{i,0}, f_{i,0}\}, \tag{B4}$$

where $U_{i,0}(I,\phi) = U_i[f_{j,0}]$. Consider that beam i experiences a small perturbation from its equilibrium distribution $\psi_i(I,\phi,\theta) = f_i(I,\phi,\theta) - f_{i,0}(I,\phi)$. The linearized equation for $\psi_i(I,\phi,\theta)$ can be obtained by subtracting Eq. (B4) from Eq. (B3) and neglecting the term $\{U_i[\psi_j],\psi_i\}$ which is higher order in ψ_i as

$$\frac{\partial\psi_i}{\partial\theta} + \nu_{i,x}\frac{\partial\psi_i}{\partial\phi} = \{U_{i,0},\psi_i\} + \{V_i, f_{i,0}\}, \tag{B5}$$

where $V_i(I,\phi,\theta) = U_i[\psi_j]$.

To solve Eq. (B5), one can convert it into a system of infinite numbers of coupled ordinary differential equations of modes by using the Fourier transformation

$$\psi_i(I,\phi,\theta) = \int_{-\infty}^{\infty} d\nu \sum_{m=-\infty}^{\infty} \psi_{i,m}(I,\nu) e^{i(m\phi-\nu\theta)}, \tag{B6}$$

where ν is the oscillation frequency of the beams and m denotes modes. The $m=1$ mode corresponds to the coherent dipole oscillation. To further simplify the problem, one may use the single-mode approximation in which only the mode with $m=1$ is kept in the linearized Vlasov equation [4]. It turns out that the use of the single-mode approximation is not only a convenience but also a necessity. Without the single-mode approximation, no effective method is available for the general solution of Eq. (B5), except for simplified models as in Ref. [21]. Substituting Eq. (B6) into Eq. (B5), multiplying $e^{-i\phi}$, and integrating ϕ over 2π on the both sides of Eq. (B5), and only keeping the $m=1$ mode, yields

$$\nu\overline{\psi_i}(I,\nu) = \nu_{i,x}\overline{\psi_i}(I,\nu) + Q_i(I)\overline{\psi_i}(I,\nu) + \int_0^{\infty} G_i(I,I')\overline{\psi_j}(I',\nu)dI', \tag{B7}$$

where $\overline{\psi_i}(I,\nu) = \psi_{i,1}(I,\nu)$,

$$Q_i(I) = \frac{1}{2\pi}\int_0^{2\pi} \frac{\partial U_{i,0}}{\partial I} d\phi, \tag{B8}$$

and

$$G_i(I,I') = \frac{\xi_{i,x}\sigma_{j,x}^2}{\pi\sqrt{2\beta_{i,x}I}}\int_0^{2\pi}\int_0^{2\pi} \frac{e^{-i\phi}\sin\phi'}{\sqrt{\beta_{i,x}I}\sin\phi - \sqrt{\beta_{j,x}I'}\sin\phi'} \times \left(2I\cos\phi\frac{\partial f_{i,0}}{\partial I} - \sin\phi\frac{\partial f_{i,0}}{\partial\phi}\right)d\phi' d\phi. \tag{B9}$$

If the equilibrium distributions are independent of ϕ such as for Gaussian beams, the imaginary term of $G_i(I,I')$ is zero. Otherwise, this imaginary term contributes a damping to the linearized Vlasov equation when $\overline{\psi_i}$ is stable or an excitation when $\overline{\psi_i}$ is unstable. If the equilibrium distributions $f_{i,0}$ are Gaussian, with a similar algebraic treatment in Ref. [4], the integrals in Eqs. (B8) and (B9) can be calculated analytically as

$$Q_i(I) = -\frac{\xi_{i,x}\sigma_{j,x}^2}{\beta_{i,x}I}(1 - e^{-\beta_{i,x}I/\sigma_{j,x}^2}), \tag{B10}$$

$$G_i(I,I') = \xi_{i,x} r_{ij} e^{-(z_i+z_j')/2}\left[\frac{\min(z_i, r_{ij}z_j')}{\max(z_i, r_{ij}z_j')}\right]^{1/2}, \tag{B11}$$

where $i=1$ or 2, $j=1$ or 2, but $i\neq j$. $z_i = \beta_{i,x}I/\sigma_{i,x}^2$, $z_j' = \beta_{j,x}I'/\sigma_{j,x}^2$, and $r_{ij} = \sigma_{j,x}^2/\sigma_{i,x}^2$.

1. Eigenfrequencies and eigenvectors of the linearized Vlasov equation

To further proceed with Eq. (B7), one may discretize the action space (I) into a mesh and solve the equation on the grids [3,4]. Let $I = l\Delta I$, where ΔI is the grid size; $l = 0, 1, 2, \ldots l_p$; and $l_p\Delta I$ is the size of the mesh. Since the distributions decay to zero quickly as I increases, a mesh that covers several $\sigma_{i,x}$ is good enough for a calculation of the coherent frequency. In order to have an accurate frequency for the lattice tune in the eigenfrequencies of Eq. (B7), however, the mesh has to be large enough so that the beam-beam interaction at $I = l_p\Delta I$ is negligible. In this study, we therefore used $l_p\Delta I = 160\,\epsilon_{i,x}$ and $\Delta I = 0.05\,\epsilon_{i,x}$, where $\epsilon_{i,x}$ is the normalized emittance of beam i. Let $\psi_i(l\Delta I,\nu) = \overline{\psi_{il}}(\nu)$. Equation (B7) can then be converted into a system of linear algebraic equations on the mesh,

$$\nu\overline{\psi_{il}} = \nu_{i,x}\overline{\psi_{il}} + Q_i(l\Delta I)\overline{\psi_{il}} + \Delta I\sum_{k=0}^{l_p} G_i(l\Delta I, k\Delta I)\overline{\psi_{jk}}, \tag{B12}$$

which leads to an eigenvalue problem

$$\mathbf{M}\vec{V} = \nu\vec{V}, \tag{B13}$$

where

$$\vec{V} = (\overline{\psi_{10}}, \overline{\psi_{11}}, \ldots, \overline{\psi_{1l_p}}, \overline{\psi_{20}}, \overline{\psi_{21}}, \ldots, \overline{\psi_{2l_p}})^T.$$

$\mathbf{M}$ is a $2(l_p+1)\times 2(l_p+1)$ matrix

$$\mathbf{M} = \begin{pmatrix} \mathbf{M}_1 & \mathbf{O}_1 \\ \mathbf{O}_2 & \mathbf{M}_2 \end{pmatrix}, \tag{B14}$$

where $\mathbf{M}_1$, $\mathbf{M}_2$, $\mathbf{O}_1$, and $\mathbf{O}_2$ are $(l_p+1)\times(l_p+1)$ matrices. Because of the single-mode approximation, $\mathbf{M}_1$ and $\mathbf{M}_2$ are diagonal matrices with the diagonal elements

$$(\mathbf{M}_i)_{kk} = \nu_{i,x} - Q_i[(k-1)\Delta I] \tag{B15}$$

and the elements of $\mathbf{O}_i$ are

$$(\mathbf{O}_i)_{kl} = G_i((k-1)\Delta I, (l-1)\Delta I), \tag{B16}$$

where $k = 1, \ldots, (l_p+1)$, $l = 1, \ldots, (l_p+1)$ and $i = 1$ or 2. If the equilibrium distributions are Gaussian, all these matrix elements in Eqs. (B15) and (B16) can be calculated analytically by using Eqs. (B10) and (B11). In the case of the HERA experiment, the equilibrium distribution of the p beam is still very close to a Gaussian but the e^+ beam is no longer a Gaussian beam (see Figs. 5 and 6). Let beam 1 and 2 be the e^+ and p beam, respectively. $\mathbf{M}_1$ and $\mathbf{O}_2$ can then be obtained analytically. The matrix elements of $\mathbf{M}_2$ and $\mathbf{O}_1$, on the other hand, have to be calculated numerically by using Eqs. (B8) and (B9) with the quasiequilibrium distribution of the e^+ beam obtained from the beam simulation.

With the eigenvalue equation in Eq. (B13), the eigenfrequencies and a set of orthogonal eigenvectors for the linearized Vlasov equation can be found numerically. If the two beams have the same lattice tune, the eigenfrequencies of Eq. (B13) are identical to that obtained in Ref. [4]. Figure 8(a) is an example of eigenfrequencies of Eq. (B13) for the case of $\nu_{1,x} = \nu_{2,x}$ and $\xi_{1,x} = \xi_{2,x}$. It shows that in the symmetrical case of beam-beam interactions, the coherent frequency [the first frequency line from the left of Fig. 8(a)] is separated from the rest of the eigenfrequencies that form a continuous band. The width of the band equals the incoherent beam-beam tune shift. The coherent frequency can therefore be easily identified in this case. Note that the coherent beam-beam tune shift

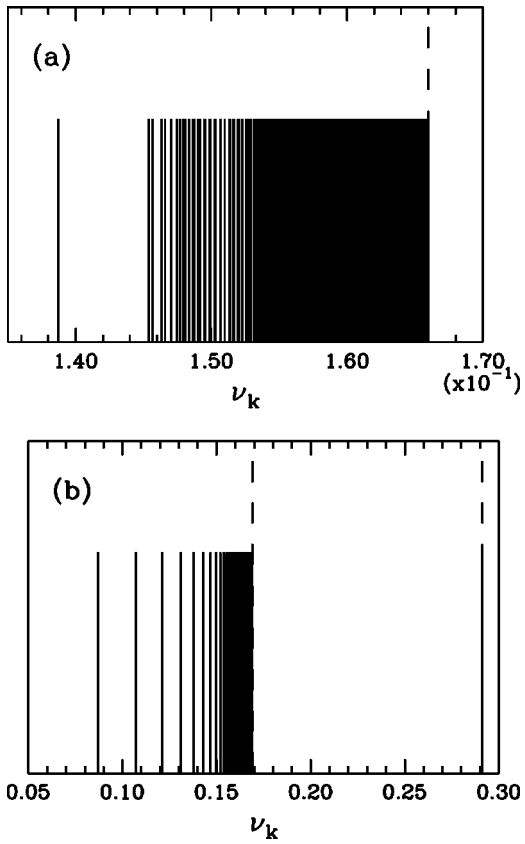

FIG. 8. Eigenfrequencies of Eq. (B13) for the case of (a) $\nu_{1,x}=\nu_{2,x}$, $\xi_{1,x}=\xi_{2,x}$ and (b) the HERA beam experiment. In (a), the dashed line marks the lattice tune that corresponds to the 0 mode. The single isolated line on the left is the coherent frequency that corresponds to a ratio of the coherent beam-beam tune shift and the total beam-beam parameter of 1.35. In (b), the dashed lines mark the lattice tunes of the e^+ beam (the left line) and p beam (the right line), respectively. The single isolated line on the right is the degenerated eigenfrequencies for the p beam and the band on the left is for the e^+ beam. The vertical axis has no physical meaning.

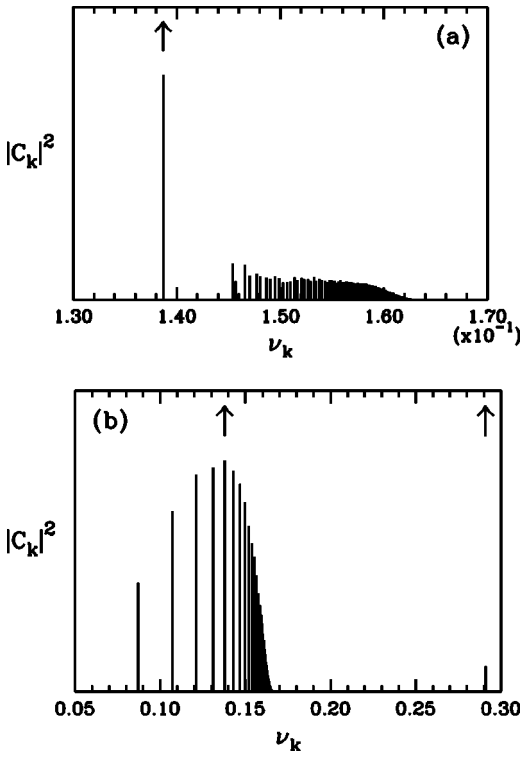

FIG. 9. $|C_k|^2$ as a function of ν_k for the cases of Fig. 8. The arrows indicate the coherent frequencies.

calculated from this coherent frequency is the same as that in Ref. [4]. The situation is more complicated when the two beams have very different lattice tunes. Figure 8(b) plots the eigenfrequencies for the case of the HERA experiment. In this case, the eigenfrequencies are divided into two groups, one for each beam. For the e^+ beam, the eigenfrequencies form a continuous band that starts at the lattice tune of the e^+ beam and has a width of the incoherent beam-beam tune shift of the e^+ beam. Because there were two IPs in the HERA experiment, the incoherent beam-beam tune shift in Fig. 8(b) is $2\xi_{e,x}=0.082$ for the e^+ beam. The characteristics of the eigenfrequencies for the p beam, in principle, is similar to that of the e^+ beam. Since the beam-beam parameter of the proton beam is very small ($\xi_{2,x}=\xi_{p,x}\sim 10^{-4}$), all the eigenfrequencies for the p beam degenerate into a single line [the first line from the left of Fig. 8(b)] that corresponds to the lattice tune of the p beam. In the case of very unsymmetrical beam-beam interactions, therefore, the coherent frequencies cannot be simply identified from the eigenfrequencies of the linearized Vlasov equation.

It should be noted that because of a very small beam-beam parameter of the p beam, during the HERA experiment no coherent beam-beam tune shift was observed on the proton beam. The matrix elements of $\mathbf{O}_2$ are very small as compared with the diagonal elements of $\mathbf{M}_1$ and $\mathbf{M}_2$. $\mathbf{O}_2$ can therefore be approximated as a zero matrix and the eigenfrequencies for the e^+ beam can be easily obtained from $\mathbf{M}_1\vec{V}_1=\nu\vec{V}_1$, where $\vec{V}_1=(\overline{\psi}_{10},\overline{\psi}_{11},\ldots,\overline{\psi}_{1l_p})^T$ is the subvector space associated with the e^+ beam. Since $\mathbf{M}_1$ is diagonalized, solving the eigenfrequencies and a set of orthogonal eigenvectors of $\mathbf{M}_1$ is trivial. The eigenfrequencies and eigenvectors obtained from $\mathbf{M}_1$ were found to be the same as that of Eq. (B13) in the subvector space associated with the e^+ beam in this case.

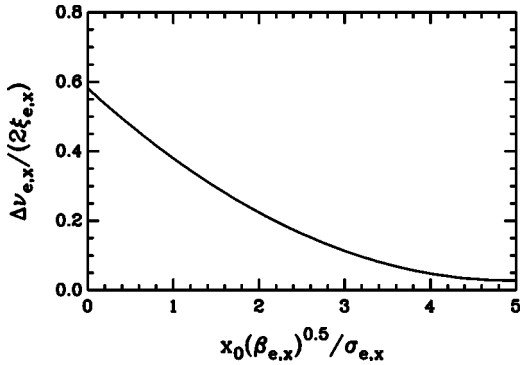

FIG. 10. Calculated coherent beam-beam tune shift by using the linearized Vlasov equation as a function of initial kick x_0 on the distribution of the e^+ beam [see Eq. (B15)] for the case of the HERA experiment at $\beta_{e,y}=1.0$ m.

2. Initial-value problem for coherent frequencies

Let $(\nu_1, \ldots, \nu_{l_p+1}, \nu_{l_p+2}, \ldots, \nu_{2l_p+2})$ and $(\vec{V}^{(1)}, \ldots, \vec{V}^{(l_p+1)}, \vec{V}^{(l_p+2)}, \ldots, \vec{V}^{(2l_p+2)})$ be the eigenfrequencies and eigenvectors of the discretized and linearized Vlasov equation where $\mathbf{M}\vec{V}^{(n)} = \nu_n \vec{V}^{(n)}$. In the HERA experiment, the lattice tunes of the two beams are very different and, therefore, the two eigenfrequency bands of Eq. (B13) are well separated [see Fig. 8(b)]. In this case, $\{\nu_n\}$ are the eigenfrequencies for the e^+ beam when $n=1, \ldots, l_p+1$ and the eigenfrequencies for the p beam when $n=l_p+2, \ldots, 2l_p+2$. In the discretized action space, the perturbation of the beam distribution $\psi_1(I, \phi, \theta)$ and $\psi_2(I, \phi, \theta)$ can be represented as a vector,

$$\vec{\psi}(\theta) = (\psi_1(0, \phi, \theta), \psi_1(\Delta I, \phi, \theta), \ldots, \psi_1(l_p \Delta I, \phi, \theta), \psi_2(0, \phi, \theta), \ldots, \psi_2(l_p \Delta I, \phi, \theta))^T.$$

With the single-mode approximation, the general solution of $\psi_1(I, \phi, \theta)$ and $\psi_2(I, \phi, \theta)$ can then be obtained from a superposition of the eigenvectors of the linearized Vlasov equation,

$$\vec{\psi}(\theta) = \sum_{k=1}^{2l_p+2} C_k \vec{V}^{(k)} e^{i(\phi - \nu_k \theta)}, \tag{B17}$$

where $\{C_k\}$ are constants and can be determined with an initial condition, $\psi_1(I, \phi, 0)$ and $\psi_2(I, \phi, 0)$. Since $|C_k|^2$ is the oscillation amplitude of the beam distributions with the frequency of ν_k, the diagram of $|C_k|^2$ versus ν_k corresponds to the frequency spectrum of the coherent oscillation. The two peaks in the $|C_k|^2 - \nu_k$ diagram, therefore, provide the coherent tunes when $\psi_1(I, \phi, 0) \to 0$ and $\psi_2(I, \phi, 0) \to 0$.

Consider a small kick that kicks beam 1 away from its equilibrium distribution $f_{1,0}(I, \phi)$, where $f_{1,0}(I, \phi)$ is known numerically from the beam-beam simulation. The initial perturbation of the beam distribution is

$$\psi_1(I, \phi, 0) = f_{1,0}(x + x_0, p_x) - f_{1,0}(x, p_x) = \sum_m g_m(I) e^{im\phi} \tag{B18}$$

and $\psi_2(I, \phi, 0) = 0$, where x_0 is the initial kick. With the single-mode approximation, $\psi_1(I, \phi, 0) \simeq g_1(I) e^{i\phi}$ and $\vec{\psi}(0) = \vec{g} e^{i\phi}$, where $\vec{g} = (g_1(0), g_1(\Delta I), \ldots, g_1(l_p \Delta I), 0, \ldots, 0)^T$. Note that the second half of the vector is all zero because beam 2 is not kicked. On the other hand, from Eq. (B17),

$$\vec{\psi}(0) = \left(\sum_{k=1}^{2l_p+2} C_k \vec{V}_k \right) e^{i\phi} = (\mathbf{V}\vec{C}) e^{i\phi}, \tag{B19}$$

where $\mathbf{V}$ is a $(2l_p+2) \times (2l_p+2)$ matrix of which the ith column is $\vec{V}_i$ and $\vec{C} = (C_1, C_2, \ldots, C_{2l_p+2})^T$. The coefficients $\{C_k\}$ can then be calculated from $\vec{C} = \mathbf{V}^{-1}\vec{g}$. It should be noted that the initial kick on the beam distributions in Eq. (B18) can be in any direction in phase space since the coherent frequency is the frequency of an infinitesimal oscillation. For near-integrable systems considered in this study, the phase-space region in the vicinity of the origin is integrable and only consists of invariant circles (tori). It is therefore isotropic. The coherent frequencies calculated were indeed found to be independent of the direction of the initial kick.

Figure 8 plots the calculated $|C_k|^2 - \nu_k$ diagrams for the symmetrical case of beam-beam interactions where $\nu_{1,x} = \nu_{2,x}$ and $\xi_{1,x} = \xi_{2,x}$ [Fig. 9(a)] and for the HERA experiment [Fig. 9(b)]. In Fig. 9(a), the peak with an arrow is the calculated coherent frequency that is the same as that in Fig. 8(a). In Fig. 9(b), the main peak indicates the calculated coherent frequency of the e^+ beam in the HERA experiment. The small peak in the lower right corner is the coherent frequency of the p beam. Figure 10 plots the calculated coherent beam-beam tune shift of the e^+ beam as a function of initial kick x_0 for the case of the HERA experiment. It shows that the calculated coherent beam-beam tune shift increases with the decrease of x_0 and converges as x_0 approaches zero. This amplitude dependence of the coherent frequency is consistent with the beam simulation. Since the coherent frequency is the frequency of an infinitesimal oscillation, the convergence of the calculated coherent frequency at $x_0 \to 0$ provides the wanted coherent frequency. As shown in our study (see Sec. IV), the linearized Vlasov equation with the single-mode approximation is a valid approach for the coherent beam oscillation with symmetrical beam-beam interactions but not with unsymmetrical beam-beam interactions.

[1] A. W. Chao and R. D. Ruth, Part. Accel. **16**, 201 (1985).
[2] J. Shi and D. Yao, Phys. Rev. E **62**, 1258 (2000).
[3] R. E. Meller and R. H. Siemann, IEEE Trans. Nucl. Sci. **28**, 2431 (1981).
[4] K. Yokoya and H. Koiso, Part. Accel. **27**, 181 (1990); KEK Report 89-14 (1989), and the references therein.
[5] K. Hirata, Nucl. Instrum. Methods Phys. Res. A **269**, 7 (1988).
[6] H. Koiso *et al.*, Part. Accel. **27**, 83 (1990).
[7] E. Keil, CERN Report, CERN-LEP-NOTE-294 (1981).
[8] A. Hofmann, in *Proceedings of the Workshop on Beam-Beam Effects in Large Hadron Colliders*, edited by J. Poole and F. Zimmermann, CERN-SL-99-039 AP (1999), p. 56.
[9] A. Piwinki, IEEE Trans. Nucl. Sci. **26**, 4268 (1979).
[10] R. Talman, CLNS-84/610 (1984).
[11] Y. Alexahin, Part. Accel. **59**, 43 (1998).
[12] M. Vogt, T. Sen, and J. A. Ellison, Phys. Rev. ST Accel. Beams **5**, 024401 (2002).
[13] M. P. Zorano and F. Zimmermann, Phys. Rev. ST Accel. Beams **3**, 044401 (2000).
[14] G. H. Hoffstaetter in *HERA Accelerator Studies 1999*, edited by G. H. Hoffstaetter, DESY HERA 00-02 (2000), p. 6.
[15] L. Jin and J. Shi, Phys. Rev. E **69**, 036503 (2004).
[16] G. H. Hoffstaetter in *HERA Accelerator Studies 2000*, edited by G. H. Hoffstaetter, DESY HERA 00-07 (2000), p. 5.
[17] M. Sands, Stanford Linear Accelerator Center Report No. SLAC-121 (1970).
[18] K. Hirata and F. Ruggiero, LEP Note 611 (1988).
[19] Y. Cai, A. W. Chao, S. I. Tzenov, and T. Taijima, Phys. Rev. ST Accel. Beams **4**, 011001 (2001).
[20] Y. Cai, private communication and also in his talk "Beam-Beam Simulation for PEP-II," PEP-II Machine Advisory Committee meeting, October 9, 2003.
[21] B. S. Schmekel, G. H. Hoffstaetter, and J. T. Rogers, Phys. Rev. ST Accel. Beams **6**, 104403 (2003).